Provided for non-commercial research and education use.
Not for reproduction, distribution or commercial use.

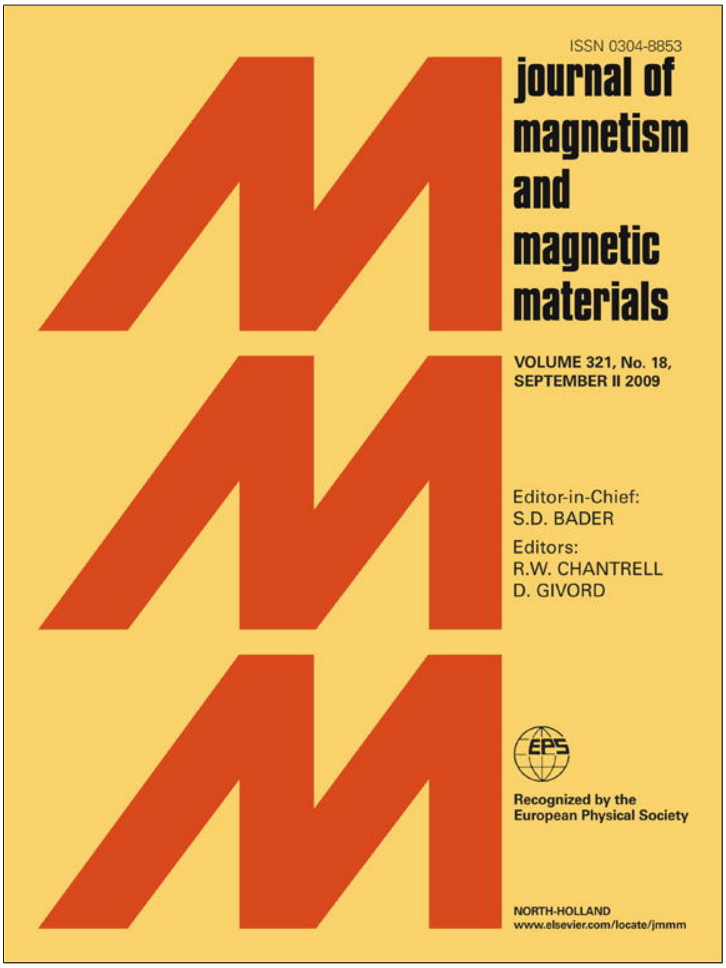

ISSN 0304-8853
journal of magnetism and magnetic materials
VOLUME 321, No. 18,
SEPTEMBER II 2009

Editor-in-Chief:
S.D. BADER
Editors:
R.W. CHANTRELL
D. GIVORD

Recognized by the
European Physical Society

NORTH-HOLLAND
www.elsevier.com/locate/jmmm

This article appeared in a journal published by Elsevier. The attached copy is furnished to the author for internal non-commercial research and education use, including for instruction at the authors institution and sharing with colleagues.

Other uses, including reproduction and distribution, or selling or licensing copies, or posting to personal, institutional or third party websites are prohibited.

In most cases authors are permitted to post their version of the article (e.g. in Word or Tex form) to their personal website or institutional repository. Authors requiring further information regarding Elsevier's archiving and manuscript policies are encouraged to visit:

http://www.elsevier.com/copyright

Journal of Magnetism and Magnetic Materials 321 (2009) 2932–2935

Contents lists available at ScienceDirect

Journal of Magnetism and Magnetic Materials

journal homepage: www.elsevier.com/locate/jmmm

Anomalous magnetization reversal mechanism in unbiased Fe/FeF$_2$ investigated by means of the magneto-optic Kerr effect

Andrea Tillmanns [a,*], Tomasz Blachowicz [b], Michael Fraune [c,1], Gernot Güntherodt [c], Ivan K. Schuller [d]

[a] FTB, Niederrhein University of Applied Sciences, Webschulstr. 31, 41065 Mönchengladbach, Germany
[b] Institute of Physics, Silesian University of Technology, Krzywoustego 2, 44100 Gliwice, Poland
[c] Physikalisches Institut IIA, RWTH Aachen University, Templergraben 55, 52056 Aachen, Germany
[d] Department of Physics, University of California, San Diego, La Jolla, CA 92093-0319, USA

ARTICLE INFO

Article history:
Received 25 January 2009
Received in revised form
14 April 2009
Available online 23 April 2009

PACS:
85.75.–d
75.60.Jk
78.20.Ls
75.70.Cn

Keywords:
Exchange bias system
Magneto-optic Kerr effect
Anisotropy
Magnetization reversal mechanism
Simulation

ABSTRACT

The coercive fields of Fe/FeF$_2$(110) bilayers above the Néel temperature of FeF$_2$ have been studied by means of the magneto-optic Kerr effect (MOKE). To distinguish the anisotropies, the longitudinal as well as the transverse magnetization components were measured and simulated. The latter allow for a conclusion about the different magnetization reversal mechanisms above and below the Néel temperature of FeF$_2$, i.e. for unbiased and exchange-biased bilayers, leading to a modified description of the magnetization reversal processes at high temperatures with explicitly forbidden local energy minima.

© 2009 Elsevier B.V. All rights reserved.

1. Introduction

There are two main issues related to today's magnetoelectronic devices which take advantage of the spin-engineered multilayer structures: one is related to the dynamical functionality and the other emphasizes the static behaviour. Both dynamical and static performance can be adjusted by a proper choice of magnetic anisotropies imposed on a layered structure. In a special case, the spins of a ferromagnetic (FM) layer can be biased in one direction only by an adjacent antiferromagnetic (AFM) layer. This is the case for a unidirectional (exchange bias, EB) anisotropy. For this purpose the exchange-coupled FM/AFM bilayers have to be field cooled to below the Néel temperature of the AFM [1–3].

Exchange bias systems can exhibit an asymmetry of the hysteresis loop for many combination of magnetic materials [2,4,5] and especially for systems with FeF$_2$ as AFM layer [6–8]. Measurements by longitudinal and transverse MOKE [9,10] showed that a broad peak on one side of the loop can be attributed to magnetization reversal by two 90° rotations via a stable intermediate state perpendicular to the saturation direction. The absence of a transverse magnetization component on the other side of the hysteresis loop can be interpreted as a non-uniform reversal, which is qualitatively consistent with theoretical predictions for a twinned EB system [11] with the magnetic field rotated with respect to the AFM easy axis.

However, while MOKE measurements are an appropriate tool to detect the longitudinal and transverse magnetization components, they are usually not suited for a quantitative determination of magnetic anisotropies. An established optical method for determining quantitatively magnetic anisotropies by measurements of anisotropy constants is, for example, Brillouin light scattering (BLS) [12]. Here, we show that the combination of transverse and longitudinal MOKE geometries, along with simple simulations, not only allows for the determination of the anisotropies, but furthermore provides a deeper insight into the magnetization reversal process for unbiased as well as exchange-biased samples.

The Fe/FeF$_2$ samples investigated in this work consist of a ferromagnetic and an antiferromagnetic layer, which exhibit an exchange bias effect after field cooling below the Néel temperature $T_N = 78.4$ K of FeF$_2$. What is proposed here, however, are MOKE tests of the magnetization reversal mechanism *at room temperature*. Although it has been shown that the Néel

---

[*] Corresponding author. Tel.: +49 2161 186 6099; fax: +49 2161 186 6013.
E-mail address: Andrea.Tillmanns@HS-Niederrhein.de (A. Tillmanns).
[1] Present address: Robert Bosch GmbH, CR/ART1, 70839 Gerlingen Schillerhöhe.

0304-8853/$ - see front matter © 2009 Elsevier B.V. All rights reserved.
doi:10.1016/j.jmmm.2009.04.046

temperature and the blocking temperature of an exchange bias system can strongly differ from bulk values for thin antiferromagnetic layers [13,14], this effect can be excluded here due to the relatively thick AFM in the system under investigation. Thus, room temperature here is high enough to exclude exchange biasing. Thus, the magnetization reversal is influenced only by the FM/AFM interface and the volume-type magnetocrystalline anisotropy fields, opposite to recent investigations on the same system at low temperatures [10]. At the same time, the coercive fields yield quantitative information about the anisotropy constants of the system at the respective temperatures.

2. Materials and methods

MOKE investigations were performed with a diode laser ($\lambda = 635\,\text{nm}$). Measurements have been carried out at 293 K using a motorized drive which enables sample rotations by 360° with a precision of $\pm 0.1^\circ$. The external magnetic field was aligned parallel to the film plane. MOKE measurements were carried out using separate longitudinal and transverse MOKE geometries to detect the corresponding magnetization components M_L and M_T, respectively. To unambiguously detect pure M_L and M_T hysteresis loops, we chose *s*-polarized light for the incident beams. On the detection side, the beams reflected from the sample passed a Glan–Thompson polarizing beam splitter. This enabled separation of the reflected beams into two orthogonally polarized beams which were focused onto two photo-diodes coupled to a bridge. Prior to each measurement, the diode bridge was balanced (difference signal = 0) using a $\lambda/2$ retarding plate. The light intensities at each diode as well as the difference signal were simultaneously measured using a lock-in amplifier.

The sample under investigation is a polycrystalline, partly textured Fe film with preferred (1 0 0) orientation coupled to epitaxial, twinned antiferromagnetic $FeF_2(1\,1\,0)$ layers. The multilayer structure was grown using molecular beam epitaxy (MBE) in the following sequence: $MgO(1\,0\,0)/FeF_2(75\,\text{nm})/Fe(12\,\text{nm})/Al(10\,\text{nm})$, with the Al layer for protection against oxidation.

Measurements have been performed at room temperature, i.e. far above the bulk Néel temperature $T_N = 78.4\,\text{K}$ of FeF_2.

3. Results and discussion

Fig. 1 shows the coercive fields of the sample under examination determined from longitudinal MOKE hysteresis loops measured at room temperature for sample angles from 0° to 360°. A fourfold symmetry can be easily recognized because of the same intensities at multiples of 90°. This is expected for a ferromagnet grown with a preferential [1 0 0] texture. Examination of the transverse magnetization component leads to the same conclusion. The transverse magnetization changes sign every 45° (grey, vertical lines in Fig. 1) which is consistent with a fourfold anisotropy and excludes the possibility of an eightfold anisotropy. Under the same conditions, BLS measurements of the surface spin wave frequency as function of sample angle between 0° and 360° (inset in Fig. 1) endorse the fourfold symmetry as well.

To quantitatively explain the experimental results, we have developed a simulation which allows the determination of coercive fields from magnetic anisotropies, using the following expression for the free energy density of the FM layer:

$$F_{ani}(\phi) = K^{(4)}\cos^2(\phi)\sin^2(\phi)\sin^4(\theta) + K^{(2)}\cos^2(\phi)\sin^2(\theta) - K_{\perp}^{(2)}\cos^2(\theta), \qquad (1)$$

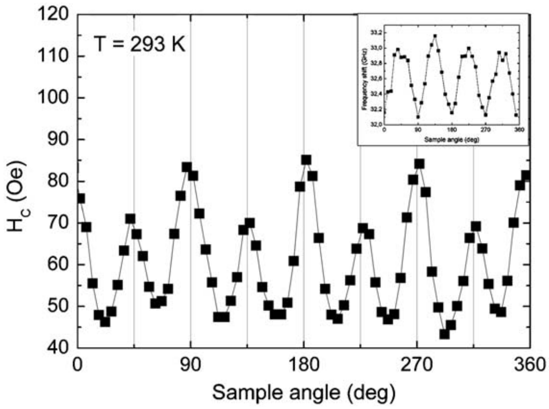

Fig. 1. Coercivity as function of sample angle, measured (full squares) with longitudinal MOKE at room temperature. Grey vertical lines: sign reversal of transverse magnetization component at 0°, 45°, 90°, …. *Inset*: surface spin wave of $Fe(1\,0\,0)/FeF_2(1\,1\,0)$ measured by BLS at room temperature as function of sample angle.

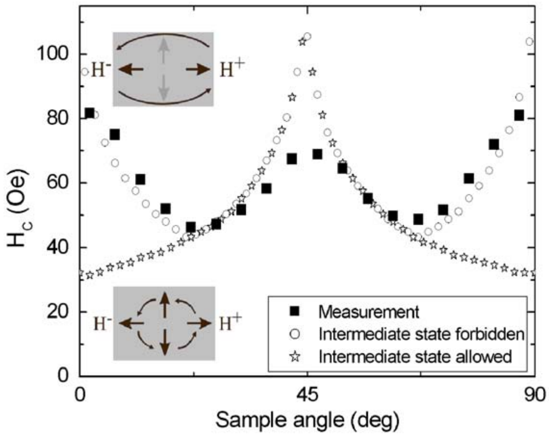

Fig. 2. Measured (full squares) and calculated H_C as function of sample angle with $K_{\parallel}^{(4)} = -1 \times 10^4\,\text{J/m}^3$. Simulated values with intermediate state allowed (explicitly forbidden) are displayed as stars (circles).

where ϕ is the in-plane sample orientation angle with respect to the magnetic field direction, θ is the angle between the surface normal and the magnetization vector direction, $K_{\parallel}^{(4)}$is the effective fourfold in-plane anisotropy constant, $K_{\parallel}^{(2)}$ the effective twofold anisotropy constant, and $K_{\perp}^{(4)}$ the effective twofold out-of-plane anisotropy constant.

The coercive fields can be calculated for all sample angles by identifying the external field which suffices to switch the magnetization over the transverse state (perpendicular to the magnetic field). For this purpose, the first derivation of the free energy density (1) is regarded. As soon as the free energy density is decreasing continuously from saturation magnetization to a state perpendicular to the external field, the longitudinal magnetization component becomes zero, and the coercive field is reached.

The theoretical coercive fields given by the simulation are depicted together with the measured values in Fig. 2. Surprisingly, the assumption that the magnetization reversal occurs by rotation of the magnetic moments via an intermediate state with $M_T \neq 0$ (i. e. by means of two 90° rotations, see lower sketch of the sample in Fig. 2) leads to simulated values (stars in Fig. 2) which do not fit the experimental findings (full squares). While the experimental data reveal maxima in the coercive fields for both the hard (0°, 90°) and easy axes (45°), the simulation which allows an intermediate state features the maximum values of the coercive fields only at the easy-axis (45°) orientations. Apparently, the usual assumption that the magnetic moments can follow the local energy minima until the magnetization reversal is completed, is not valid in the sample under investigation.

However, the experimental observation can easily be explained by using the same model, modified to explicitly forbid the intermediate states (local energy minima) with the magnetization perpendicular to the external field (see upper sample sketch and open circles in Fig. 2). Hence, the magnetization reversal occurs only when a complete 180° rotation is energetically allowed. For this purpose, the coercive fields are calculated now as the fields for which the free energy density is continuously dropping from one saturation magnetization to the other. The difference between both the reversal mechanisms is visualized in Fig. 3. If the intermediate state is *allowed* (middle panel), the coercive fields are defined by the magnetization reversal to this intermediate state (at ~32 Oe). The magnetization reversal to the final state – after a complete 180° rotation – can only be seen by a very small change in the longitudinal magnetization component (at ~95 Oe) which normally cannot be recognized in an experiment. However, if the intermediate state is *explicitly forbidden* (lower panel), the coercive field is defined by the external field allowing for a complete 180° rotation of the magnetization, which is much larger than the coercivity obtained before.

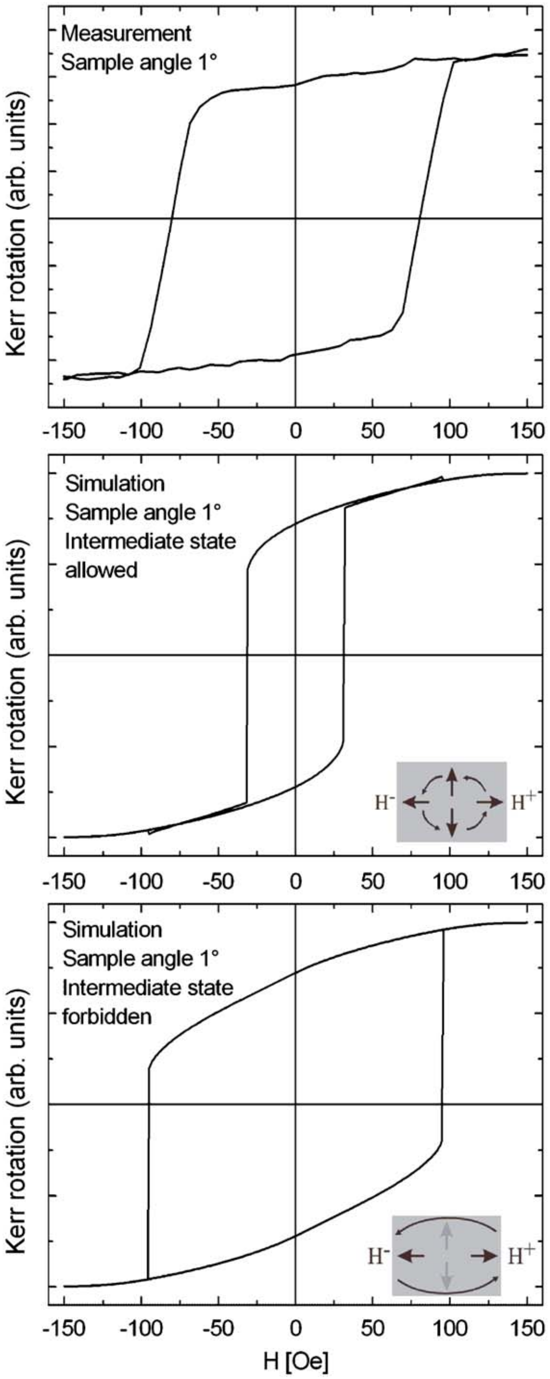

Fig. 3. Measured (upper panel) and simulated longitudinal hysteresis loop for the intermediate state allowed (middle panel) and explicitly forbidden (lower panel).

Since the simple macrospin simulation does not consider the possibility of overcoming small energy barriers and, on the other hand, ignores the statistic distribution of the anisotropy axes which can be expected in real samples, the calculated maxima in Fig. 2 are naturally sharper and higher than the experimental ones. Adjusting the calculated coercive fields at fixed θ to the measured values in a broad angular region leads to the anisotropy constants $K_{\parallel}^{(4)} = -1\times10^5\,\mathrm{erg/cm^3} = -1\times10^4\,\mathrm{J/m^3}$, $K_{\parallel}^{(2)} = K_{\perp}^{(2)} = 0$ and $\theta = 90°$.

To decide whether the claimed 180° rotations with explicitly forbidden local energy minima are identical with domain wall nucleations and propagations, the transverse magnetization components were also analyzed (Fig. 4). While magnetization reversal via domain wall processes would not exhibit a distinct transverse magnetization component (transverse moments in a domain wall are too small to explain the experimental findings), in Fig. 4 pronounced transverse magnetization peaks can be found which are due to a fraction of the magnetic moments, which rotate during magnetization reversal.

An estimate of the transverse peak height can be obtained from calculation of the energy barrier for a *clockwise* magnetization rotation under the assumption that the magnetization rotation occurs *counter-clockwise* and vice versa, since the probability of a magnetic moment rotating *clockwise* is the larger, the higher the energy barrier for a *counter-clockwise* rotation is. These values differ for both magnetization reversal types with the intermediate state explicitly forbidden or allowed, since the heights of the energy barriers for the magnetization rotation in the "forbidden" rotational direction differ. The measured peak height follows the

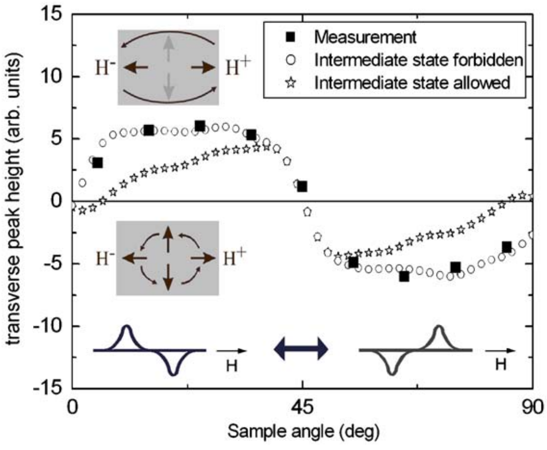

Fig. 4. Measured (full squares) and calculated height of the transverse peak (positive sign meaning peak on the left side of the hysteresis loop being positive) with $K_{\parallel}^{(4)} = -1\times10^4\,\mathrm{J/m^3}$. Simulated values with intermediate local energy minima allowed (explicitly forbidden) are displayed as stars (circles). *Bottom insets*: sketches of typical transverse magnetization components near the left and right coercive fields of the hysteresis loop for ferromagnets with Stoner–Wohlfarth-type magnetization rotation.

estimated values for a 180° rotation with no intermediate state allowed.

Nevertheless, domain wall processes are a sufficient explanation for this finding. Assuming that a fraction of the magnetization reverses via domain wall nucleation and propagation, these domains would induce large internal fields which could superpose the minima of the anisotropy fields. The latter are perpendicular to the saturation magnetization, leading to higher energies in these angular regions, and thus influence the reversal process of the other moments which reverse via rotation.

4. Conclusions

We have shown that in the system Fe/FeF_2 the FM magnetization reversal at temperatures above the AFM Néel temperature occurs via 180° rotations with intermediate energy minima being explicitly forbidden. The same behaviour can be found, e.g., in Fe/MnF_2 [15], suggesting that this finding is not limited to only very special systems. This result is in contrast to measurements obtained well below the Néel temperature where the exchange-biased system exhibits transverse magnetization components. The latter can be simulated assuming magnetization reversal via two 90° rotations over an intermediate energy state [9,10].

Generally, we have demonstrated that by measuring the longitudinal and transverse magnetization components, we can obtain effective values of the anisotropy constants. In addition, we have provided direct evidence for different types of the magnetization reversal mechanisms for unbiased and exchange-biased FM/AFM systems. Further investigation should reveal a balance between both reversal mechanisms at a temperature close to the AFM Néel temperature because measurements at different temperatures between 20 and 100 K have shown a smooth change from high temperature behaviour – as described in this paper – to the longitudinal and transverse magnetization components expected for an exchange bias system with fourfold anisotropy [16]. Since a broad temperature range below the Néel temperature is influenced by these two opposite mechanisms, knowledge about the reversal mechanism, obtained far away from the Néel temperature of the AFM transition, proves to be informative for studies of exchange-biased bilayers.

Acknowledgements

Work at UCSD supported by the US-DOE. I K. S thanks the A. von Humboldt Foundation and RWTH Aachen University for their support and hospitality during a sabbatical visit.

References

[1] W.H. Meiklejohn, C.P. Bean, Phys. Rev. 102 (1956) 1413–1414.

[2] J. Nogués, I.K. Schuller, J. Magn. Magn. Mater. 192 (1999) 203–232.

[3] A.E. Berkowitz, K. Takano, J. Magn. Magn. Mater. 200 (1999) 552–570.

[4] R. Jungblut, R. Coehoorn, M.T. Johnson, J. aan de Stegge, A. Reinders, J. Appl. Phys. 75 (1994) 6659–6664.

[5] W.C. Cain, M.H. Kryder, J. Appl. Phys. 67 (1990) 5722–5724.

[6] J. Nogués, D. Lederman, T.J. Moran, I.K. Schuller, K.V. Rao, Appl. Phys. Lett. 68 (1996) 3186–3188.

[7] J. Nogués, D. Lederman, T.J. Moran, I.K. Schuller, Phys. Rev. Lett. 76 (1996) 4624–4627.

[8] D. Lederman, J. Nogués, I.K. Schuller, Phys. Rev. B 56 (1997) 2332–2335.

[9] A. Tillmanns, S. Oertker, B. Beschoten, G. Güntherodt, C. Leighton, Ivan K. Schuller, J. Nogués, Appl. Phys. Lett. 89 (2006) 202512.

[10] A. Tillmanns, S. Oertker, B. Beschoten, G. Güntherodt, J. Eisenmenger, Ivan K. Schuller, Phys. Rev. B 78 (2008) 012401.

[11] B. Beckmann, K.D. Usadel, U. Nowak, Phys. Rev. B 74 (2006) 054431.

[12] P. Baumgart, B. Hillebrands, G. Güntherodt, J. Magn. Magn. Mater. 93 (1991) 225–228.

[13] P.J. van der Zaag, Y. Ijiri, J.A. Borchers, L.F. Feiner, R.M. Wolf, J.M. Gaines, R.W. Erwin, M.A. Verheijen, Phys. Rev. Lett 84 (2000) 6102–6105.

[14] M.J. Carey, A.E. Berkowitz, J. Appl. Phys. 73 (1993) 6892–6897.

[15] A. Tillmanns, Ph.D. thesis, RWTH Aachen University (2005) 41; 〈http://darwin.bth.rwth-aachen.de/opus3/volltexte/2006/1352/〉.

[16] A. Tillmanns, Ph.D. thesis, RWTH Aachen University (2005) 41, p. 70.〈http://darwin.bth.rwth-aachen.de/opus3/volltexte/2006/1352/〉.